

# Experimental Modeling of the Continuous Casting Process of Steel Using Low Melting Point Metal Alloys—the LIMMCAST Program

Klaus TIMMEL, Sven ECKERT, Gunter GERBETH, Frank STEFANI and Thomas WONDRAK

Forschungszentrum Dresden-Rossendorf (FZD), MHD Department, 01314 Dresden, Germany.

(Received on February 5, 2010; accepted on May 17, 2020)

This paper presents the new experimental facility LIMMCAST which was designed for modeling fluid flow and transport processes in the continuous casting of steel. The facility operates at temperatures of 200–400°C by using the low melting point alloy SnBi. The main parameters of the facility, including the dimensions of the test sections, will be given. The resultant possibilities with respect to flow investigations in the tundish, in the submerged entry nozzle, and in the mould will be discussed. Over the period of assembling and commissioning the LIMMCAST facility, the small-scale set-up Mini-LIMMCAST was employed which uses the alloy GalnSn that is liquid at room temperatures. At this precursory facility an experimental program was started which is focused on quantitative flow measurements in the mould and in the submerged entry nozzle (SEN). The Ultrasound Doppler Velocimetry (UDV) and the Contactless Inductive Flow Tomography (CIFT) were applied to determine the flow structure within the mould. First experimental results will be presented here for a single and a two-phase flow in which argon gas bubbles were injected at the inlet of the SEN. According to the concept of the electromagnetic brake the impact of a DC magnetic field on the emergent jet flow from the SEN has been studied.

KEY WORDS: continuous casting; liquid metal model experiments; flow measurements; two-phase flow; electromagnetic brake.

## 1. Introduction

Owing to a persistent quest for better product quality and higher productivity of the continuous casting of steel, the flow control in the tundish and in the mould as well as the initial solidification control in the mould become more and more important. A multitude of numerical simulations have been carried out (see for example<sup>1–4</sup>), but in most instances the reliability of the numerical results is only insufficiently validated by accompanying experimental activities. The use of water models is reasonable and allows for applying a number of well-established measuring methods. However, a generalization of those results to liquid metal flows has to be considered as questionable because the true values of flow parameters (Re, Pr, Gr, Ha, *etc.*) are difficult to meet. In many cases, *e.g.* for liquid metal flows with strong temperature gradients, for two-phase flows, and of course for applications of electromagnetic fields, the flow phenomena cannot be modeled correctly by means of water experiments.

Related experimental studies with liquid metals are rather scarce until now. Several plant trials were carried out<sup>5,6</sup> to study the efficiencies of electromagnetic brakes (EMBR) in the real casting process. Because of the lack of suitable measuring techniques for liquid steel at 1500°C such trials cannot provide reliable quantitative data about

the magnetic field effect on the flow in the mould. Only rough information might be achieved by visual observations of the surface velocity or by the application of imprecise mechanical metering devices.

As for model experiments with low melting point metals, previous studies have been made by a Japanese group employing simplified mercury set-ups.<sup>7,8</sup> Using this model, Vives-type sensors were applied to investigate the effects of a DC magnetic field<sup>7</sup> or an electromagnetic stirrer<sup>8</sup> on the fluid flow, respectively. With our work we want to pursue the strategy of cold liquid metal models the main value of which consists in the capability to obtain quantitative flow measurements with a reasonable spatial and temporal resolution within a liquid metal flow. New ultrasonic techniques for measuring the velocity in liquid metal flows have been established during the last decade allowing for a satisfying characterization of flow quantities in the considered temperature range until 300°C.<sup>9</sup> In the same period, a new electromagnetic method for the flow visualization has been developed. In the present study we will show how the Ultrasound Doppler Velocimetry (UDV) and the Contactless Inductive Flow Tomography (CIFT) can be applied for an instantaneous determination of the flow pattern inside the mould. We will also show first results concerning the influence of applied magnetic fields on the flow structure, and the two-phase flow in which argon gas bubbles were in-

jected at the inlet of the SEN.

## 2. Experimental Facility LIMMCAST

A new Liquid Metal Model for Continuous Casting of steel (LIMMCAST) is available at FZD. The scientific program of this experimental facility aims to model the essential features of the various flow fields that are of relevance for the continuous casting of steel, namely the flow field in the tundish, in the submerged entry nozzle (SEN), and in the mould cavity. At a later stage, the solidification of the material in the strand is also to be investigated. The facility has been designed and assembled during the last two years. The operation has been started in March 2009 with the first filling of the facility with SnBi. After verification of the instrumentation, the process measuring and control technology, the commissioning phase has been finished in September 2009.

**Figure 1** shows a simplified scheme of the continuous casting process. A schematic diagram of the LIMMCAST facility is displayed in **Fig. 2**. All components to be in contact with the liquid metal are made of stainless steel. The low melting point alloy Sn<sub>60</sub>Bi<sub>40</sub> is used as model liquid. The liquidus temperature of 170°C allows for an operation of the facility in a temperature range between 200 and 400°C. An overall heating power of about 200 kW is installed at the outer wall of the piping system and the components to achieve the operating temperature. **Table 1** shows a comparison between the essential material properties of Sn<sub>60</sub>Bi<sub>40</sub> and liquid steel. The melt inventory is stored in two vessels with a capacity of 250 L for each vessel. For operation the alloy is melted and pushed with argon from the storage vessels into a piping system. The present situation of the facility comprises two test sections. Test section I, which contains the tundish, the SEN and the mould, will be used for physical modeling of the continuous casting process. The investigations will be explicitly focused on the behaviour of the isothermal melt flow. A fur-

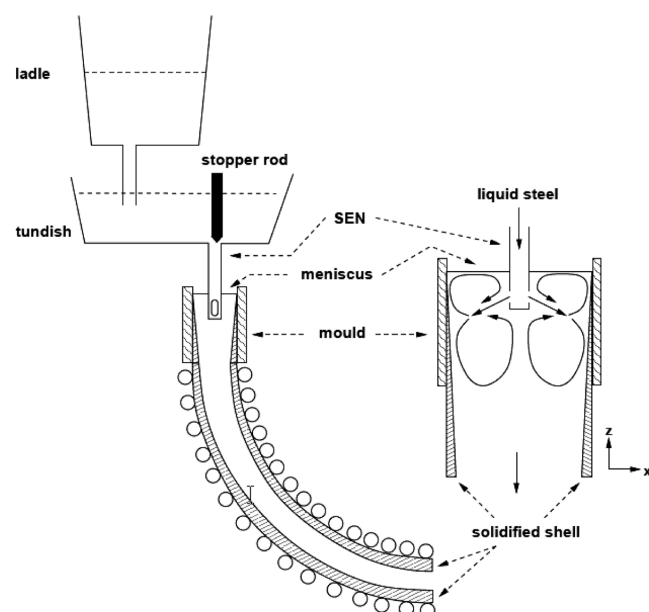


**Fig. 1.** Schematic representation of the continuous casting process of steel and the flow field in the mould.

ther test section has been installed as a closed channel with a straight test section and serves for material tests or verifications of various measuring techniques. A third test section, at which a solidification of the strand will become possible, will be realized in future.

An overall view of the LIMMCAST facility is shown in **Fig. 3**. An electromagnetic pump<sup>10)</sup> is used to convey the liquid metal into the tundish. The flow rate is measured by an electromagnetic flow meter.<sup>11)</sup> **Figure 4** displays the test section with tundish, SEN and mould. From the tundish the melt pours through a pipe with an inner diameter of 35 mm

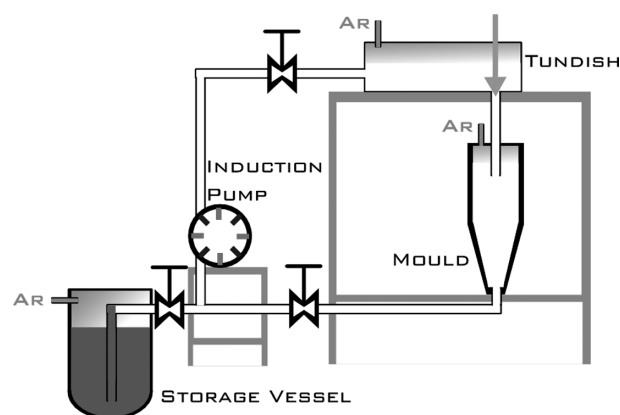


**Fig. 2.** Schematic view showing the main components of the LIMMCAST facility.

**Table 1.** Material properties of liquid steel (at 1 600°C), SnBi (at 200°C) and GaInSn (at room temperature).

	Steel	Sn60Bi40	Ga68In20Sn12
Liquidus (°C)	1510	170	10.5
Solidus (°C)	1480	138	
Density $\rho$ (kg/m <sup>3</sup> )	7900	8250	6360
Viscosity $\nu$ (10 <sup>-6</sup> m <sup>2</sup> /s)	0.85	0.19	0.34
Electrical. cond. $\sigma_{el}$ (10 <sup>6</sup> /Ωm)	0.77	1.05	3.2
Thermal cond. $\lambda$ (W/Km)	25	35	39
Surface tension $\sigma$ (N/m)	1.6	0.46	0.53



**Fig. 3.** Overall view of the LIMMCAST facility.

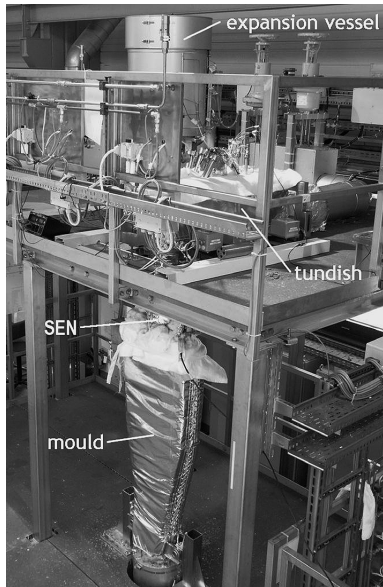


Fig. 4. Photograph of the test section with the tundish and the mould at the LIMMCAST facility.

into the mould which has a rectangular cross section of  $400 \times 100 \text{ mm}^2$ . The flow rate is controlled by a stopper rod. Argon gas can be injected into the melt flow through this stopper rod. In the first instance, different kinds of magnetic fields, in particular DC fields and electromagnetic stirrers, will be installed at the mould region. However, respective studies considering the magnetic field impact are also foreseen for the flow in the tundish and the SEN. Special adapters at the lid of the mould allow for a direct access of various kinds of measuring techniques to the liquid metal in the mould. For instance, flow velocities will be determined using the UDV method. High temperature sensors equipped with acoustic wave guides<sup>12)</sup> will be attached to the free surface of the melt to determine the vertical component of the liquid velocity. Further adapters are available for visual inspections of the free surface. Moreover, local probes can be positioned inside the melt to measure velocity fluctuations<sup>13)</sup> or void fraction distributions in case of gas bubbling.<sup>14)</sup> Actually, the recent developments in measurement techniques for liquid metal flows<sup>9)</sup> represent the essential basis for the construction of our “cold” liquid metal models. The almost complete measurement of the related single- or two-phase flows is the main objective in order to provide a better understanding of those flows and to serve for the validation of numerical simulations.

Though the EM stirring in the mould seems promising for future applications in steel casting too,<sup>15)</sup> our measuring program will start with systematic investigations of the influence of a horizontal DC magnetic field on the flow inside the mould. This situation is governed by the following non-dimensional parameters (see Table 1 for the material properties):

Reynolds number  $Re = \frac{UL}{\nu}$  .....(1)

Hartmann number  $Ha = BL \sqrt{\frac{\sigma}{\rho\nu}}$  .....(2)

Magnetic interaction parameter  $N = \frac{\sigma LB^2}{\rho U}$  .....(3)

Taking a typical pouring velocity  $U$  of 1.5 m/s and the mould width  $L$  of 100 mm as a basis, the LIMMCAST facility with the test section described above will cover a Reynolds number range up to  $10^6$ . A DC magnetic field with maximum field strength  $B$  of 0.7 T will be applied at the mould resulting in a maximum Hartmann number of approximately 1 800 and an interaction parameter of about 4 at  $U=1.5$  m/s. In parallel to the DC field studies, corresponding investigations with AC field stirrers are in preparation.

3. Mini-LIMMCAST: a Small-scale GaInSn Facility

During the construction and commissioning period of the large scale LIMMCAST facility, the small-scale set-up Mini-LIMMCAST was employed which uses the eutectic alloy GaInSn that is liquid at room temperatures. At this set-up we started a preliminary experimental program which is focused on quantitative flow measurements in the mould and in the submerged entry nozzle (SEN). This way we expected to gain valuable experiences for the detailed design and the operation of the larger LIMMCAST facility.

3.1. Experimental Set-up

Figure 5 shows a schematic drawing of the Mini-LIMMCAST facility. A stainless steel cylinder serves as the tundish which contains about 3.5 L of the GaInSn alloy. Material properties of GaInSn can be found in Table 1. The melt is discharged through a Plexiglas tube with inner diameter of 10 mm into the mould with a rectangular cross section of  $140 \times 35 \text{ mm}^2$  (also made from Plexiglas). Two nozzle ports with an oval cross section (vertical dimension 18 mm) are situated approximately 80 mm below the free surface in the mould. From the mould the liquid metal flows over a dam into a storage vessel. The vertical position of the dam controls the free surface level in the mould. An electromagnetic pump conveys the melt from the vessel back into the tundish. The experiments presented here were performed in a discontinuous mode, *i.e.* after filling the tundish with the melt the stopper rod was lifted to drain the fluid into the mould. During this process the liquid level of both the tundish and the mould were monitored using a laser and an ultrasonic distance sensor, respectively. The liquid flow rate has been derived from the descent of the surface level in the tundish. A schematic view of the section comprising the outlet of the tundish with the stopper rod, the SEN and the mould can be seen in Fig. 6.

During the two-phase flow experiments argon gas was injected at the tip of the stopper rod. Gas flow rates were adjusted in a wide range between 50 and 500 cm<sup>3</sup>/min by means of a mass flow controller (MKS1359C, MKS Instruments). Pressure measurements were carried out within the gas feeding system using the pressure sensor PS001V (Turck Ind. Autom.).

For modelling the influence of an electromagnetic brake (EMBR) on the flow, a DC magnet is attached to the mould that produces a transverse magnetic field with a maximum field strength of 0.31 T. Measurements of the field strength

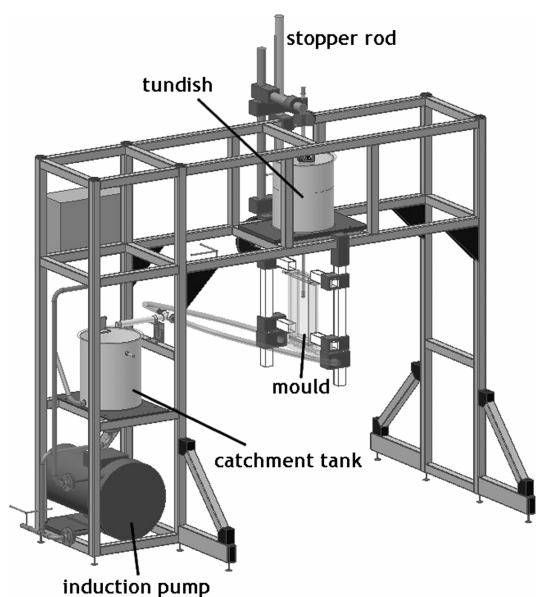


Fig. 5. Schematic drawing of the small-scale GaInSn model Mini-LIMMCAST.

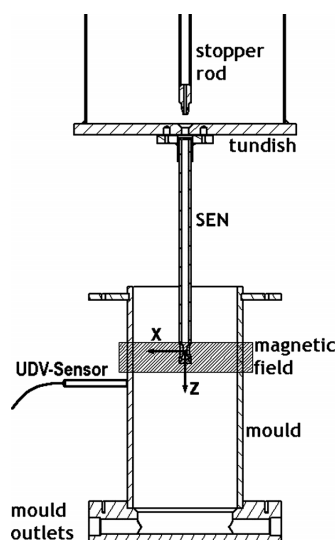


Fig. 6. Detailed view showing the tundish with the stopper rod, the SEN and the mould (Mini-LIMMCAST).

showed that the field is homogenous between the pole faces within a tolerance of about 5%. The pole faces of the magnet cover the wide side of the mould completely. The vertical extension of the pole shoes is 40 mm, whereas the position of the upper edge of the pole faces coincides with the nozzle outlet (see Fig. 6).

The ultrasound Doppler velocimetry (UDV) was used for measuring the fluid velocity in the mould. This method is based on the pulse-echo technique and delivers instantaneous profiles of the local velocity along the ultrasonic beam and can be applied to attain experimental data from a bulk flow in opaque liquids.<sup>16)</sup> The measuring volume consists of a series of disks lined up concentrically along the propagation direction of the ultrasound. In the last twenty years the UDV technique became an accepted method for flow investigations in various liquid metals (see for instance<sup>9,12,17)</sup>). In the present study we have applied the DOP2000 velocimeter (model 2125, Signal Processing SA,

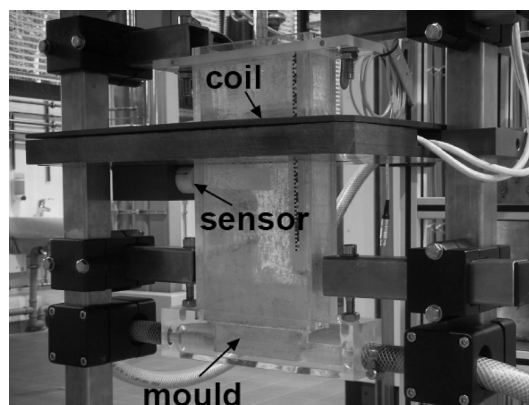


Fig. 7. Photograph of the mould showing the CIFT configuration with the coil and one magnetic field sensor.

Lausanne) equipped with up to ten 4 MHz transducers (TR0405LS, acoustic active diameter 5 mm). The internal multiplexer of the DOP2000 has been used for a sequential acquisition of data from all sensors with an overall scan rate of 5 Hz. Ten transducers were arranged within a vertical line array which was attached at the outer wall of the mould and located at the midsection of the narrow side. The distance between two adjacent transducers was 10 mm. Figure 6 shows exemplarily the mounting of one transducer at the outer wall of the mould. The horizontal alignment of the ultrasonic sensor allows for the measurement of the horizontal velocity component along the  $x$ -direction. Respective velocity profiles were recorded at the midsection along the wide side of the mould between the side wall and the submerged entry nozzle.

The Contactless Inductive Flow Tomography (CIFT) relies on measuring the flow induced perturbations of an applied magnetic field. These externally measured induced magnetic fields are utilized for inferring the three-dimensional velocity field in the fluid volume quite similar as electric currents in the human brain are reconstructed by Magnetoencephalography. A detailed description concerning the theoretical background of the velocity reconstruction, including the use of appropriate regularization techniques for the solution of the inverse problem can be found in.<sup>18,19)</sup> For applying CIFT to Mini-LIMMCAST, a rectangular coil with 14 windings was mounted around the mould at the height of the SEN outlets as shown in Fig. 7. The coil is fed with 15 A producing a mainly vertical magnetic field of approx. 1 mT in the mould region where the flow field is to be determined. It should be noticed that, by utilizing the divergence free constraint, CIFT is able to reconstruct also the vertical velocity component although this does not induce any electric current in a vertical magnetic field. Fluxgate sensors (Foerster) which are capable to detect weak induced magnetic fields on the background of a much stronger applied field were chosen for the measurements. The sensors are directly mounted at the corpus of the coil in order to avoid variations of the signal due to dislocations between coil and sensor. The sensor positions are vertically adjustable. More details about the measuring configuration and the procedure to infer the velocity can be found in.<sup>20)</sup>

### 3.2. Experimental Results

#### 3.2.1. Measurements of the Flow Pattern in the Mould

The flow structure in the upper part of the mould is of particular interest because it affects considerably the quality of the produced steel slab. For instance, asymmetric flows caused by uneven discharge from the SEN can generate unwanted level oscillations leading to the entrapment of mould flux and the transport of nonmetallic inclusions into the solidifying strand. In view of such problems, an online-monitoring of the flow structure would be highly desirable. The application of traditional flow measuring techniques is inhibited by the opaqueness and the high temperature of the liquid steel. Thus, the application of CIFT offers an attractive alternative.

Before applying CIFT to Mini-LIMMCAST, numerical simulations were performed first to figure out the optimal coil size and position as well as the best locations for the sensors. As a result, the coil was installed at the height of the jet in order to achieve a maximum of the induced magnetic field. These induced fields were then measured at the middle of the narrow face of the mould. By moving the sensor, measurements were performed at 36 vertical positions. In order to ensure invariant conditions for every measurement, the flow rate of the liquid metal in the SEN, the vertical position of the meniscus and the position of the stopper rod were recorded.

In **Fig. 8(a)** we compare the simulated induced magnetic field with the field that was measured at 36 positions along the height of the narrow face. The velocity field that we infer from these measured fields is then depicted in **Fig. 8(b)**. The jet from the ports of the SEN and the double-roll structure can be clearly identified in the reconstructed flow field. Note that the impingement point of the jet is characterized by a change in the sign of the measured flow-induced magnetic field.

Using the ultrasound Doppler method with ten ultrasonic transducers, we have also recorded profiles of the horizontal velocity component directed along the wide side of the mould. **Figure 9** contains the resulting time-averaged plot of the horizontal velocity component which reveals the intensity, shape and impinging point of the jet. The results of those ultrasonic measurements agree reasonably with the horizontal velocity components obtained with CIFT (see *Ref. 20*)).

#### 3.2.2. The Impact of a Transverse DC Magnetic Field

Various designs and miscellaneous operation conditions have been proposed to apply DC magnetic fields for flow control in the continuous casting mould. In this section we consider the situation that a horizontal magnetic field is imposed to the mould flow as described in the previous chapter. This set-up corresponds to the configuration of a ruler-type electromagnetic brake (EMBR).

**Figure 10** displays the two-dimensional pattern of the horizontal velocity obtained by UDV for the case of a field intensity of 0.31 T. The application of the magnetic field provokes a strong recirculating flow at the upper part of the nozzle outlet. The inclination angle of the jet becomes flat. Compared to the situation without magnetic field, as shown in **Fig. 9**, the impingement point at the opposite side wall is

shifted upwards by about 20 mm. The intensity of the velocity within the jet is only slightly reduced.

The arrangement of the ultrasonic transducers has been modified to measure the velocity distribution in the narrow, horizontal cross section of the mould. Three transducers were positioned at the midsection, two of them at a distance of 13 mm at either side of the central sensor. The vertical position corresponds to the bottom end of the SEN ( $z=19$  mm). For the case without magnetic field, **Fig. 11(a)** shows a distinct peak of the velocity at the midsection, whereas an equalization of the velocity distribution can be observed in the direction of the magnetic field as shown in **Fig. 11(b)**.

Consecutive plots of subsequent velocity profiles recorded by one transducer yield a quasi spatio-temporal pattern at that position. Such spatio-temporal plots of the velocity obtained at a position inside the jet 19 mm beneath the nozzle outlet can be seen in **Fig. 12**. The particular velocity profiles have been drawn along the ordinate whereas the abscissa is determined by the running time. The amplitude of the velocity is represented by the colour map. **Figure 12(b)** reveals large scale oscillations of the local velocity in the magnetic field which probably arise from an alternating up- and downturn of the jet. These oscillations cause a reduction of the time-averaged values of the velocity at that particular position, however, a slowdown of the velocity fluctuations due to the magnetic field effect cannot be observed.

Such findings might be astonishing on the first view, but can be understood by considering the generic problem of an initially axisymmetric jet, which is affected by a uniform, transverse magnetic field (for a detailed discussion see Davidson<sup>21</sup>). The imposed field causes regions of reverse flow on both sides of the central jet. Furthermore, an elongation of the jet cross-section parallel to the field lines occurs. These general features with respect to a reorganization of the flow pattern were also found recently in an experimental study with respect to a bubble-driven liquid metal flow in a transverse magnetic field.<sup>22</sup>) An outcome was the feature that a static magnetic field may give rise to non-steady, non-isotropic large-scale flow perturbations. Similar tendencies can be observed in our simplified continuous casting model. Thus, the preliminary flow measurements presented here did not confirm the expectation of a smooth reduction of the velocity fluctuations at the nozzle outlet due to the magnetic field. This problem requires further investigation, because the concept of an EMBR in the continuous casting process relies on a general damping effect of the applied magnetic field. A continuation of the measurements is foreseen in future in order to obtain more data concerning temporal and spatial flow properties.

#### 3.2.3. Two-phase Flow Inside SEN and Mould

In steel casting, argon gas is injected into the steel flow through the SEN in order to avoid clogging. Ingress of air through the walls of the SEN is prevented by high pressure inside the stopper rod<sup>23</sup>) and the SEN. Moreover, the argon bubbles are supposed to drag alumina particles into the mould. The complex gas-liquid flows within the SEN and the mould have been addressed by several studies using numerical simulations and water modeling. The numerical

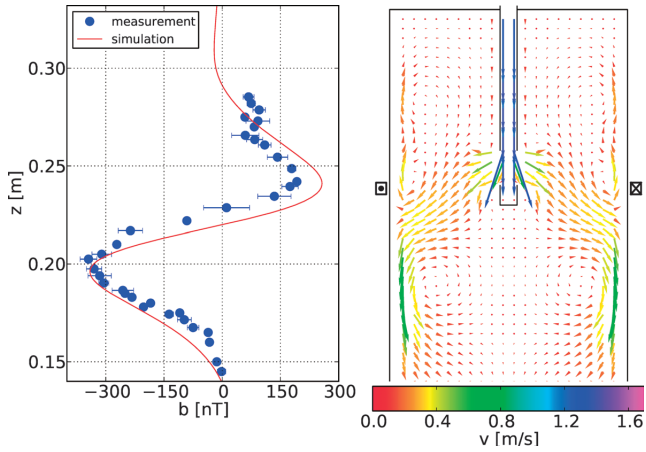


Fig. 8. Measurements of the induced magnetic field along the narrow face of the mould (left) and the flow pattern reconstructed by CIFT (right).

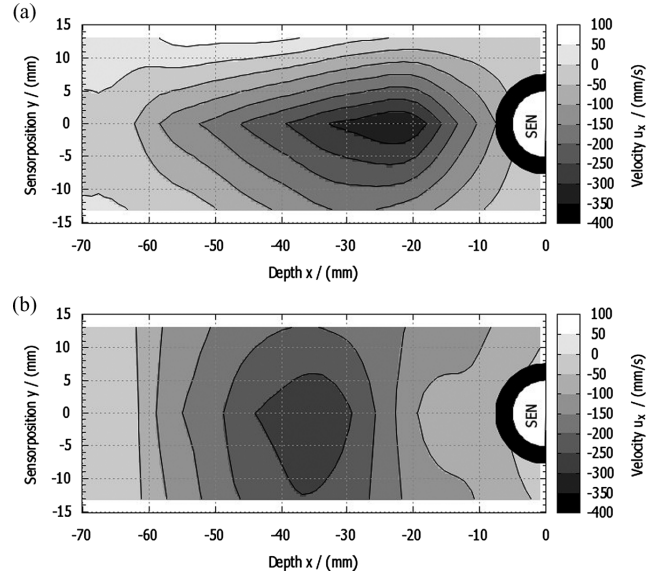


Fig. 11. UDV measurements of the horizontal flow at the nozzle outlet (horizontal arrangement of 3 transducers,  $z=19$  mm): (a) without magnetic field, (b)  $B=0.31$  T.

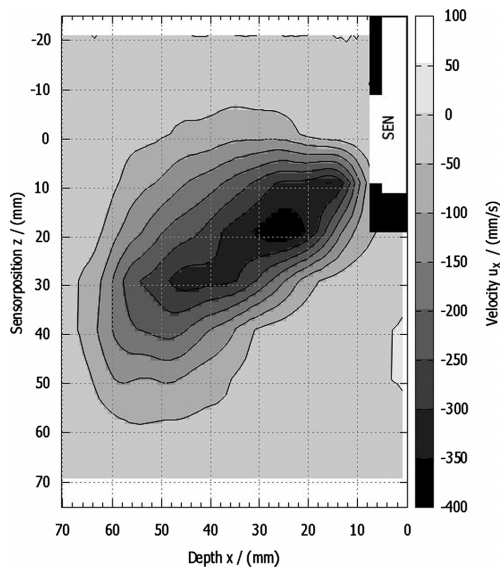


Fig. 9. UDV measurements of the time-averaged, horizontal flow (vertical arrangement of 10 transducers,  $B=0$ , midsection of the narrow mould side).

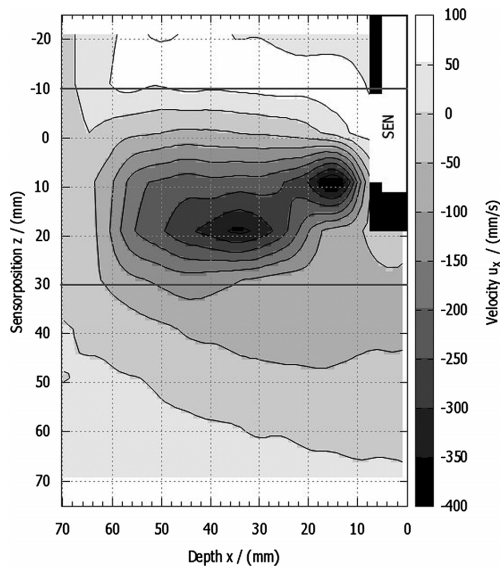


Fig. 10. UDV measurements of the time-averaged, horizontal flow under the influence of a horizontal DC magnetic field with  $B=0.31$  T (vertical arrangement of 10 transducers, midsection of the narrow mould side).

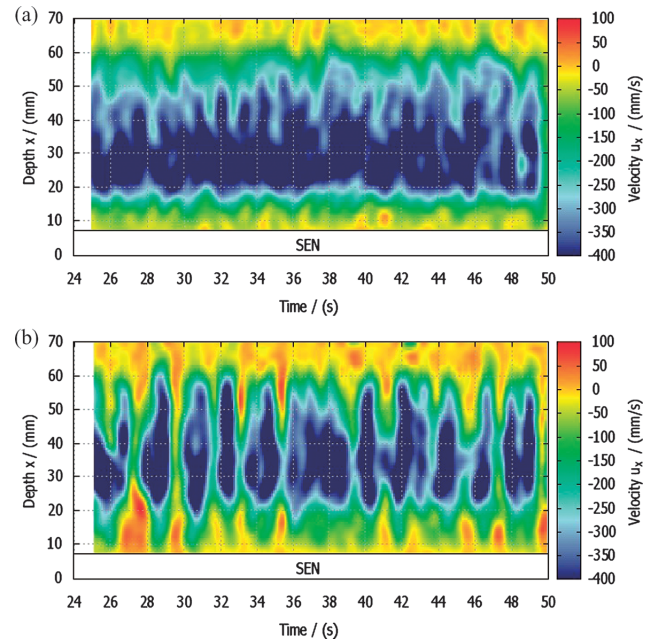


Fig. 12. Spatio-temporal plots of the horizontal flow at the nozzle outlet (sensor 5 located at  $z=19$  mm): (a) without magnetic field, (b)  $B=0.31$  T.

simulations consider mostly dispersed bubbly flows and show a considerable influence of bubble sizes on both flow structure and transport phenomena.<sup>24)</sup> The dynamics of a downward two-phase flow inside the SEN was investigated in water models.<sup>25,26)</sup>

Respective experiments with gas-liquid metal two-phase flows are scheduled for the LIMMCAST facility. Important questions concern the flow regime in the SEN, the size and the spatio-temporal distribution of the gas bubbles. The mechanism of bubble formation is very sensitive to the geometry of the gas injector and the ambient flow conditions. The contact angle between the metallic melt and the refractory in a gas atmosphere is a further key parameter in

determining the bubble size. Neither the inner diameter nor the outer bore of the nozzle controls the bubble formation. The bubble detach when the gas film growing from the injection point reaches a critical thickness where the buoyancy force overcomes the surface tension force. Such specific conditions for bubble formation can only be reproduced by a liquid metal model. First experiments showed that not all the gas injected forms bubbles within the SEN. In all likelihood, gas films were formed around the stopper rod and a part of the gas escapes along the stopper rod towards the free surface in the tundish.

First two-phase experiments were performed at Mini-LIMMCAST. Data sets were recorded for the pressure at the gas injection point and the levels of the liquid metal surface in the tundish and the mould, respectively. The monitoring of the free surface level in the tundish allows for the calculation of the liquid flow rate during the experiment. The level in the mould is measured as the distance from the upper mould edge to the liquid metal surface, *i.e.* a decrease of the respective curve in Fig. 13 represents an increase of the surface level in the mould. Figure 13(a) shows a typical experimental run without gas injection. The stopper rod is closed at the beginning of the record. After lifting the stopper rod the inflowing liquid metal causes a compression of the gas column in the SEN indicated by a temporary pressure increase. Afterwards, a negative pressure dominates owing to the pull of the falling liquid. The measured value returns to the ambient pressure after closing the stopper rod because the facility is not hermetically sealed. The analysis of the level decline in the tundish yields a liquid flow rate of 0.102 L/s corresponding to a liquid velocity of about 1.3 m/s in the nozzle. The oscillations of the free surface in the mould after closing the stopper rod are caused by the inertia of the liquid.

Figure 13(b) contains a corresponding plot obtained from an experiment with a gas flow rate of 2.5 cm<sup>3</sup>/s. Here, the gas injection was started before opening the stopper rod. The initiation of the gas flow produces an increase of the pressure followed by periodic oscillations in the pressure curve which can be related to the release of individual bubbles into the mould. Higher pressure oscillations at lower frequency can be observed in case of the flowing liquid metal what probably indicates the formation of larger gas slugs in the SEN. Corresponding oscillations of the mould level appear with a slight time offset if these gas slugs leave the metal melt in the mould. The flow regime changes abruptly about 15 s after opening the stopper rod. The oscillations disappear and the liquid flow rate increases leading to a higher mould level. Our measurements cannot doubtless clarify if a transition to a dispersed bubbly flow occurred at that moment. Another explanation concerns the leakage of the gas in the tundish along the stopper rod. Increasing the gas flow rate to a value of 3.3 cm<sup>3</sup>/s leads to a continuous slug flow showing pronounced oscillations of both the pressure curve and the mould level as displayed in Fig. 13(c).

#### 4. Summary and Concluding Remarks

Cold liquid metal models appear as an important tool for the experimental investigation of many open questions in

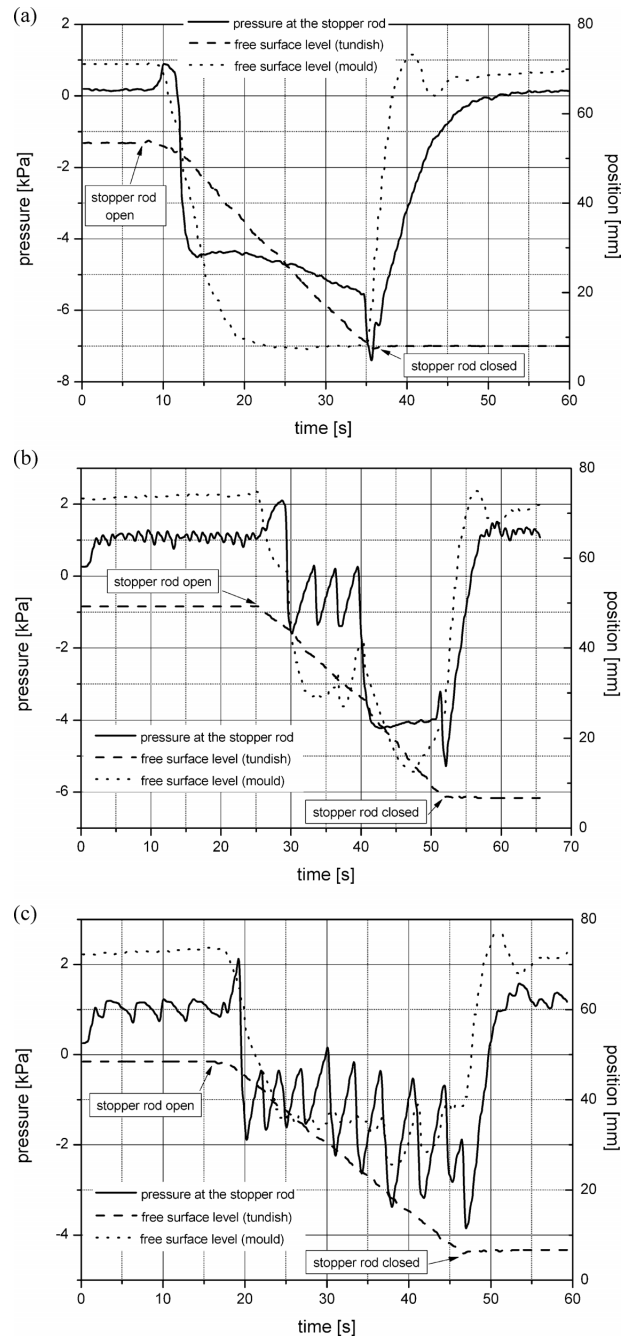


Fig. 13. History of pressure at the stopper rod, free surface level in tundish and mould, respectively: (a)  $Q_{\text{gas}} = 0$ , (b)  $Q_{\text{gas}} = 2.5 \text{ cm}^3/\text{s}$  and (c)  $Q_{\text{gas}} = 3.3 \text{ cm}^3/\text{s}$ .

steel casting. Moreover, these model experiments can provide valuable experimental data for the validation of numerical flow simulations. The LIMMCAST facility at FZD is now available for respective investigations at scales being comparable to the realistic continuous casting process. The consideration of various possibilities of electromagnetic flow control comprising both DC and AC magnetic fields will be a main issue in the experimental program. Besides the investigation of fluid flow and transport processes the facility will be used to develop and test measuring techniques and components for the real industrial process. Future plans concern the installation of a further test section which will allow for a solidification of the strand. Electromagnetic stirrers will be used here below the mould region

to cause a forced flow inside the solidifying melt. The consequences of different ways of electromagnetic stirring on the resulting microstructure in the strand will be analyzed.

First preliminary experiments have been carried out at the Mini-LIMMCAST facility focusing on the mould flow and its modification by applied transverse magnetic fields or argon injection. The Ultrasound Doppler Velocimetry (UDV) and the Contactless Inductive Flow Tomography (CIFT) have been successfully applied to determine the flow structure in the mould. Both techniques have been shown to be capable to provide valuable experimental data for comparison with numerical predictions. Future work will also be oriented on further steps towards an industrial application of the flow measurements. For CIFT, this could mean to replace the additionally applied magnetic field by the field of the electromagnetic brake as it is in the process. A particular complication for the applicability of CIFT in a real caster is the oscillation of the copper mould. Future investigations will try to deal with this problem by filtering out the corresponding signal.

The impact of a DC magnetic field on the outlet flow from the submerged entry nozzle (SEN) has been studied. A striking outcome was the feature that a static magnetic field may give rise to non-steady, non-isotropic large-scale flow perturbations. The flow measurements presented here did not confirm the expectation of a smooth reduction of the velocity fluctuations at the nozzle outlet due to the magnetic field. This problem requires further investigation, because the concept of an EMBR in the continuous casting process relies on an overall damping effect of the applied magnetic field.

Two-phase flow experiments using an injection of argon gas through the stopper rod delivered strong indication for the occurrence of a slug flow inside the SEN manifested by pronounced simultaneous, coherent oscillations of the pressure at the injection point and the liquid metal level in the mould. Further systematic experiments are necessary to figure out the occurrence of different flow regimes in the SEN depending on the ratio of liquid and gas flow rates. The instrumentation will be extended to directly detect the gas bubbles inside the SEN and in the mould. Electrical as well as ultrasonic methods are considered to serve this purpose.

### Acknowledgements

The research is supported by the Deutsche Forschungsgemeinschaft (DFG) in the framework of the SFB 609 "Electromagnetic Flow Control in Metallurgy, Crystal Growth and Electrochemistry" and by European Commission under contract 028679 (project "MAGFLOTOM"). This financial support is gratefully acknowledged by the au-

thors. Furthermore, the authors wish to express their thanks to the Research Technology Department of FZD, namely J. Claussner, R. Schlenk and J. Voigtländer, for their valuable contribution to the design and realization of the LIMMCAST facility and to D. Lucas, X. Miao and A. Peyton for fruitful discussions with respect to aspects of the two-phase flow.

### REFERENCES

- 1) B. G. Thomas and L. Zhang: *ISIJ Int.*, **41** (2001), 1181.
- 2) K. Takatani, K. Nakai, N. Kasai, T. Watanabe and H. Nakajima: *ISIJ Int.*, **29** (1989), 1063.
- 3) B. Li and F. Tsukahashi: *ISIJ Int.*, **46** (2006), 1833.
- 4) K. Cukierski and B. G. Thomas: *Metall. Mater. Trans.*, **39B** (2008), 94.
- 5) P. Gardin, J.-M. Galpin, M.-C. Regnier and J.-P. Radot: *Magneto-hydrodynamics*, **32** (1996), 189.
- 6) K. H. Moon, H. K. Shin, B. J. Kim, J. Y. Chung, Y. S. Hwang and J. K. Yoon: *ISIJ Int.*, **36** (1996), S201.
- 7) H. Harada, T. Toh, T. Ishii, K. Kaneko and E. Takeuchi: *ISIJ Int.*, **41** (2001), 1236.
- 8) K. Okazawa, T. Toh, J. Fukuda, T. Kawase and M. Toki: *ISIJ Int.*, **41** (2001), 851.
- 9) S. Eckert, A. Cramer and G. Gerbeth: *Magneto-hydrodynamics—Historical Evolution and Trends*, ed. by S. Molokov, R. Moreau, H. K. Moffatt, Springer-Verlag, Berlin, Heidelberg, New York, (2007), 275.
- 10) I. Buceniaks: *Magneto-hydrodynamics*, **36** (2000), 181.
- 11) D. Buchenau, G. Gerbeth and J. Priede: *Proc. of the 6th Int. Conf. on EPM*, eds. by G. Gerbeth, S. Eckert, Y. Fautrelle, Dresden, (2009), 383.
- 12) S. Eckert, G. Gerbeth and V. I. Melnikov: *Exp. Fluids*, **35** (2003), 381.
- 13) A. Cramer, K. Varshney, T. Gundrum and G. Gerbeth: *Flow Meas. Instrum.*, **17** (2006), 1.
- 14) S. Eckert, G. Gerbeth and O. Lielausis: *Int. J. Multiphase Flow*, **26** (2000), 45.
- 15) P. H. Dauby and S. Kunstreich: *ISSTech 2003 Conf. Proc.*, Indianapolis, Vol. 1, ISS Publication, Warrendale, PA, (2003), 491.
- 16) Y. Takeda: *Nucl. Eng. Des.*, **126** (1991), 277.
- 17) Y. Takeda: *Nucl. Technol.*, **79** (1987), 120.
- 18) F. Stefani and G. Gerbeth: *Meas. Sci. Technol.*, **11** (2000), 758.
- 19) F. Stefani, T. Gundrum and G. Gerbeth: *Phys. Rev. E*, **70** (2004), 056306.
- 20) T. Wondrak, V. Galindo, G. Gerbeth, T. Gundrum, F. Stefani and K. Timmel: *Meas. Sci. Technol.*, **21** (2009), 045402.
- 21) P. A. Davidson: *J. Fluid Mech.*, **299** (1995), 153.
- 22) C. Zhang, S. Eckert and G. Gerbeth: *J. Fluid Mech.*, **575** (2007), 57.
- 23) U. Sjöström, M. Burty, A. Gaggioli and J. P. Radot: *81st SteelMaking Conf.*, Toronto, ISS Publication, Warrendale, PA, (1998), 63.
- 24) H. Bai and B. G. Thomas: *Metall. Mater. Trans.*, **32B** (2001), 253, 269.
- 25) R. Sanchez-Perez, R. D. Morales, M. Diaz-Cruz, O. Olivares-Xometl and J. Palafox-Ramos: *ISIJ Int.*, **43** (2003), 637.
- 26) A. Ramos-Banderas, R. D. Morales, R. Sanchez-Perez, L. Garcia-Demedices and G. Solorio-Diaz: *Int. J. Multiphase Flow*, **31** (2005), 643.